Sensors and Materials, Vol. 34, No. 4 (2022) 1287–1296
MYU Tokyo

S & M 2891

Ejection Fraction Measurement and Regional Wall Motion Abnormality Assessment Using Deep-learning Neural Networks in Left Ventriculography

Shan-Bin Chan,[1] Yuan-Chun Lai,[2] Wei-Ting Chang,[3] Kuo-Ting Tang,[3] Ming-Shih Huang,[2] Zhih-Cheng Chen,[3] and Yung-Yao Chen[1*]

[1]Dept. Electronic and Computer Engineering, National Taiwan University of Science and Technology, No. 43, Sec. 4, Keelung Rd., Taipei City 106, Taiwan (R.O.C.)
[2]Open AI Fab Inc., Room 437, Building E, No. 19-11, Sanchong Rd., Taipei City 115, Taiwan (R.O.C.)
[3]Cardiovascular Division, Chi-Mei Medical Center, No. 901, Zhonghua Rd., Yongkang Dist., Tainan City 710, Taiwan (R.O.C.)

(Received July 4, 2021; accepted September 30, 2021)

Keywords: ejection fraction, regional wall motion abnormalities, deep learning, neural networks, left ventriculography, semantic segmentation, image classification

In this research, an X-ray flat panel detector is adopted as an image collection sensor for evaluating left ventricular systolic functions. Typically, left ventriculography (LVG) is conducted in the end-diastolic and end-systolic areas by clinicians, which is time-consuming, and the calculated ejection fraction (EF) varies among clinicians. We propose two novel methods for EF measurement and regional wall motion abnormality (RWMA) assessment through LVG. Our methods can automatically segment the end-diastolic and end-systolic areas for clinicians and perform EF measurement and RWMA assessment in real time. Semantic segmentation neural networks were implemented for EF measurement, and image convolution neural networks were implemented in RWMA recognition. LVG images were collected by clinicians, but the data set labeling procedure was not performed by clinicians. This method may reduce the need for medical doctors in the data set labeling procedure. Using the proposed methods, EF measurement and RWMA assessment were performed with high accuracy.

1. Introduction

Ejection fraction (EF) is the volumetric fraction of blood ejected from a heart with each heartbeat. EF and regional wall motion abnormality (RWMA) are indicators of the effectiveness of heart pumping. Transthoracic echocardiography is widely adopted for EF measurement and RWMA assessment, but left ventriculography (LVG) is the gold standard for EF measurement and RWMA diagnosis. LVG is an invasive procedure that leaves a small wound in the patient's body, whereas transthoracic echocardiography is noninvasive. Most patients choose transthoracic echocardiography for EF measurement and RWMA assessment. However, the low image quality of transthoracic echocardiography, obesity, lung disease, and chest deformity decrease the accuracy of EF measurement. Although the invasive procedure is a disadvantage of LVG, it more

*Corresponding author: e-mail: yungyaochen@mail.ntust.edu.tw
https://doi.org/10.18494/SAM3503

ISSN 0914-4935

accurately performs EF measurement and RWMA diagnosis. In this study, we proposed two neural network methods for EF measurement and RWMA assessment. The semantic segmentation neural network method is implemented for EF measurement, and an image convolution neural network classifier is implemented for RWMA assessment. Typically, EF measurement is conducted by clinicians, and the calculated EF varies among clinicians. Our proposed EF measurement method is automatic, efficient, and highly accurate. Additionally, our proposed method reduces manpower (medical doctor) requirements in the data set labeling procedure. We also proposed an image convolution neural network classifier for RWMA assessment, where we reused the semantic segmentation end-diastolic area and end-systolic area results in the LVG image in the EF measurement for RWMA classification. The proposed method achieved high sensitivity and specificity in RWMA diagnosis.

The remainder of this paper is organized as follows. In Sect. 2, we outline the related research. In Sect. 3, we introduce our proposed methods for data set collection, EF measurement, and RWMA assessment. In Sect. 4, we present our accuracy results and detail the use of the visual explanation technique termed class activation mapping (CAM)[1] analysis. Finally, we provide a discussion and our conclusions in Sects. 5 and 6, respectively.

2. Related Research

EF is widely adopted for measuring heart pumping efficiency and classifying heart failure types.[2] Typically, transthoracic echocardiography is adopted for EF measurement, but cardiac magnetic resonance imaging, cardiac computed tomography,[3,4] nuclear-medicine-based approaches (gated SPECT and radionuclide angiography),[5,6] and LVG are also used to measure EF.[7,8]

According to the 2016 European Society of Cardiology Guidelines,[9] acute and chronic heart failures are divided into three categories. LVG EF of ≥50% is classified as normal or preserved EF, LVG EF in the range of 40 to 49% is classified as mid-range reduced EF, and LVG EF of <40% is classified as reduced EF.

Cardiovascular diseases are also diagnosed by implementing deep-learning neural networks. A 3D convolutional neural network is employed to estimate and differentiate preserved EF through echocardiographic imaging.[10] A segmentation neural network has been proposed for left ventricle detection in echocardiographic images. Kim *et al.* proposed a UNet semantic segmentation neural network for left ventricle detection.[11] A neural edge detector method is also used to extract left ventricular contours using LVG.[12]

RWMAs are defined as regional abnormalities in patients with heart disease. Echocardiography is widely used for RWMA assessment. Huang *et al.* proposed a deep-learning neural network for RWMA recognition through echocardiography.[13] They proposed three models for RWMA assessment. The first model generates the best image of four major views from echocardiography images (LAX, SAX, A4C, and A2C). The second model employs the semantic segmentation neural network approach for the segmentation of each wall. The third model combines two sets of images from the first and second models and performs the final prediction for RWMA assessment.

Deep-learning neural network research on EF measurement and RWMA assessment has focused on echocardiographic images. In this study, we adopted LVG images for deep-learning neural network application. A semantic segmentation neural network is a popular algorithm for finding contours and areas of objects.[14–16] Here, a semantic segmentation algorithm is adopted for finding end-diastolic and end-systolic areas and EF measurement, and an image classification neural network is adopted for RWMA assessment.

3. Methods

In this study, two deep-learning neural network methods were employed to measure EF and classify RWMA. In the following sections, we introduce the data set collection procedure, EF measurement method, and RWMA classification method.

3.1 Data set collection

We prepared two data sets for the EF deep-learning and RWMA assessment models. To prepare the data set for the EF measurement deep-learning model, we collected patient LVG video images. LVG produces a set of sequential video images stored in dicom format. To collect the training data set, image extraction from an LVG video was required. A package for working with dicom files, called Pydicom, was adopted to extract the images from the dicom files. Each extracted LVG image was 512 × 512 pixels. For each patient, approximately 100 LVG images were extracted.

The polygonal annotation tool labelme[17] was used to annotate the training data set. For each extracted LVG image, we annotated only the area affected by the contrast medium. Only one class was annotated: the contrast medium area versus the non-contrast medium area (background). Figure 1 shows the annotation tool and annotated polygon of the contrast medium area.

To prepare the RWMA model data set, we identified the end-diastolic and end-systolic areas for each patient and calculated the stroke area as the difference between the end-diastolic and end-systolic areas for RWMA model training. In accordance with the five myocardial segments

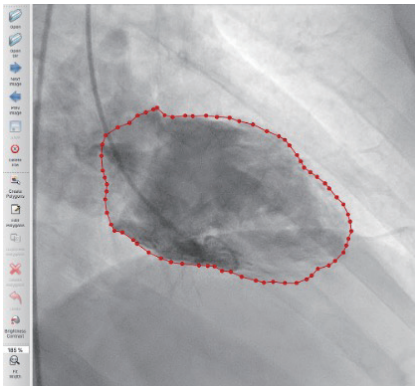

Fig. 1. (Color online) Contrast medium area annotated by labelme.

in right anterior oblique LVG (RAO-LVG), we divided the training data set into four classes, namely, apical anterior (LAD distal lesion), basal (RCA or LCX), septal (LAD proximal), and normal. Myocardial segments 234, 23, and 3 were classified as apical anterior segments. Myocardial segments 345, 45, and 5 were classified as basal segments. Myocardial segment 12 was classified as a septal segment. Figure 2 shows the five myocardial segments in RAO-LVG and Fig. 3 shows the stroke areas.

Finally, 5140 images were annotated for the EF measurement model training data set, and 258 images were annotated for the RWMA model training data set.

3.2 EF measurement model

UNet[18] with EfficientNetB4[19] was used as the backbone of the deep-learning neural network model for the EF measurement model. We also employed the MaskRCNN[20] model for EF measurement. UNet with EfficientNetB4 exhibited a high level of accuracy and mean intersection over union (mIoU) in EF measurement. Figure 4 shows the deep-learning neural network layers implemented in this research.

LVG images were extracted from patient dicom files, and semantic segmentation prediction was conducted for each LVG image. After applying semantic segmentation inferences for each LVG image, we identified the end-diastolic area followed by the end-systolic area. Because the calculation of EF required the end-diastolic and end-systolic volumes instead of areas, an area-to-volume conversion formula was required. The EF measurement formulas are shown in Eqs. (1)–(3), where SV denotes the stroke volume, EDV denotes the end-diastolic volume, and ESV denotes the end-systolic volume.

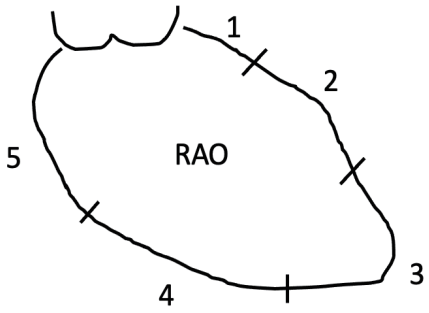

Fig. 2. Five myocardial segments in RAO-LVG.

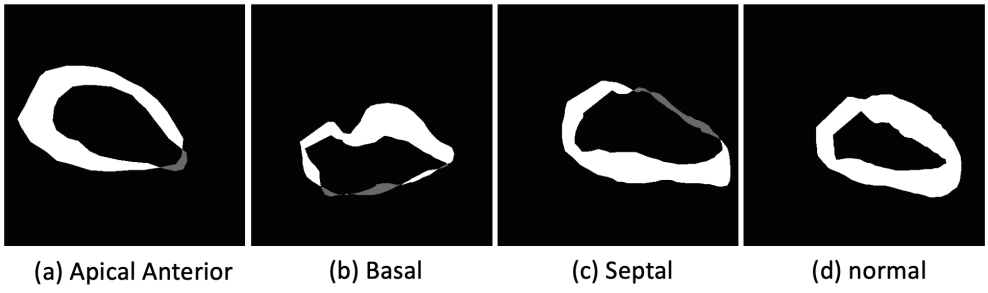

Fig. 3. LVG stroke area classes.

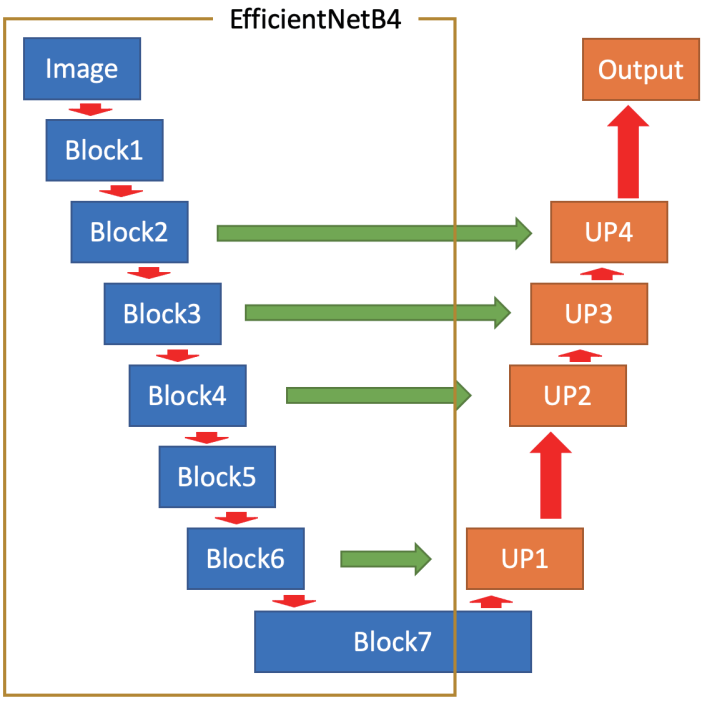

Fig. 4. (Color online) EfficientNetB4 + UNet model layers.

$$SV = EDV - ESV \tag{1}$$

$$EF = \frac{SV}{EDV} \times 100\% \tag{2}$$

$$EF = \frac{EDV - ESV}{EDV} \times 100\% \tag{3}$$

According to Eq. (4), the maximum contour length of the area (diameter) L was required in addition to the area. The enclosing circle method shown in Fig. 5 was implemented to calculate L. Upon substituting Eq. (4) into Eq. (3), the EF formula was transformed into Eq. (5), where d denotes end-diastolic and s denotes end-systolic. Finally, EF can be obtained from the end-diastolic area, the end-systolic area, the maximum contour length of the end-diastolic area, and the maximum contour length of the end-systolic area.

$$V = (8A^2)/(3\pi L) \tag{4}$$

$$EF = \frac{(8A_d^2/3\pi L_d) - (8A_s^2/3\pi L_s)}{(8A_d^2/3\pi L_d)} = \frac{(A_d^2/L_d) - (A_s^2/L_s)}{(A_d^2/L_d)} \times 100\% \tag{5}$$

Fig. 5. (Color online) Identification of the enclosing circle and diameter *L*.

3.3 RWMA assessment model

Because of the similarities among the RWMA images, we concluded that the same abnormalities were present in the same myocardial segments. Therefore, the classification model EfficientNetB3 was adopted in the RWMA assessment. Only the apical anterior, basal, septal, and normal classes were included in the classifier training.

The stroke area images calculated as the difference between the end-diastolic and end-systolic areas were employed for RWMA classifier model training. Finally, we implemented the model visual explanation technique called CAM to identify the areas on which the RWMA model was focused.

4. Results

Two evaluation methods were implemented. In the first model, a semantic segmentation neural network was adopted as the inference model for EF measurement. The mIoU value was also used for evaluation. In the second model, a classification neural network was employed as the inference model for RWMA assessment. Evaluation methods for recall, precision, sensitivity, and specificity were included in this model.

Two segmentation neural networks were used in the evaluation procedure, namely, MaskRCNN and EfficientNetB4 + UNet. In total, 5140 LVG images were included in the data set, and 10% of the LVG images were spliced as testing data. Examples of inference results are shown in Fig. 6.

The MIoU evaluation results from MaskRCNN and EfficientNetB4 + UNet are included in Table 1. The mIoU values of MaskRCNN and EfficientNetB4 + UNet were 0.8942 and 0.9215, respectively. Therefore, EfficientNetB4 + UNet was more accurate than MaskRCNN.

Typically, clinicians calculate EF measurements, but EF results vary among clinicians. Therefore, no absolute EF value exists for a patient. EF measurement results with ±10% error rates are considered reliable. In our study, 54 cases were employed to measure accuracy. Table 2 shows the EF measurement accuracy with different error rates. EfficientNetB4 + UNet was more accurate than MaskRCNN.

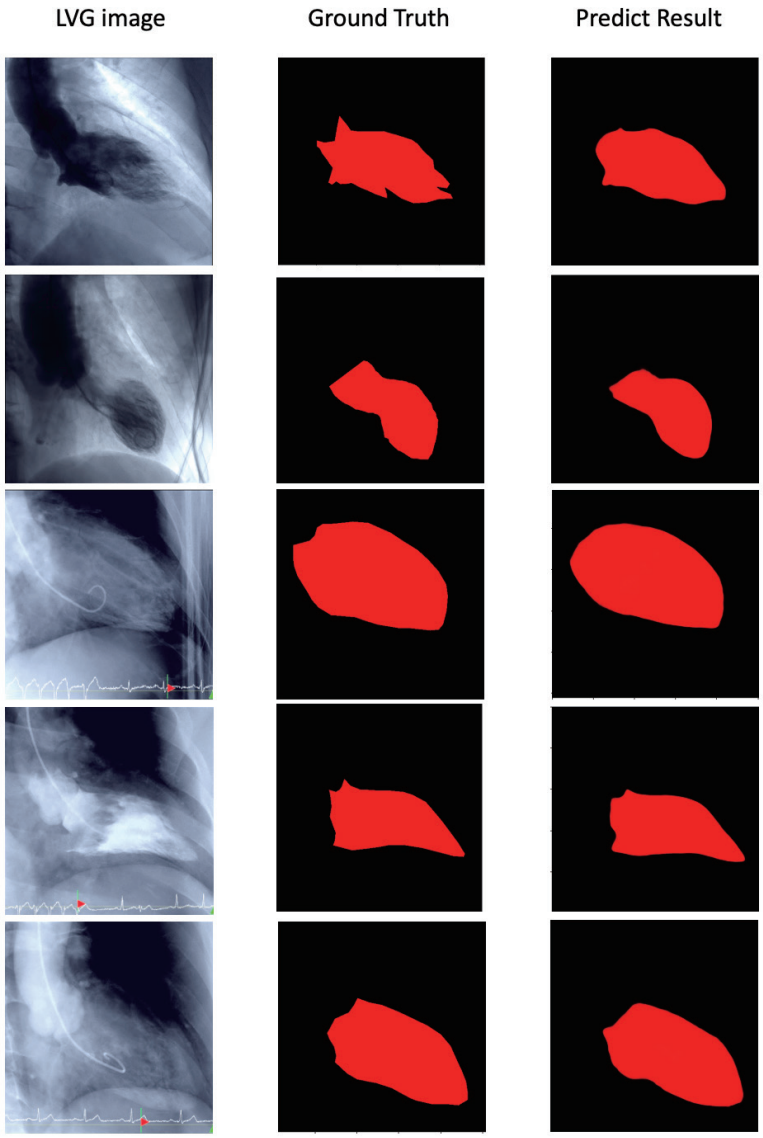

Fig. 6. (Color online) Examples of LVG images and semantic segmentation prediction results.

Table 1
MIoU evaluation results.

Model Name	mIoU
Mask R-CNN	0.8942
EfficientNetB4 + UNet	**0.9215**

Table 2
EF measurement accuracy with different error rates.

Model Name	Error < 10% (cases)	Error > 10% (cases)	Accuracy (%)	Error < 15% (cases)	Error > 15% (cases)	Accuracy (%)
Mask R-CNN	23	31	42.6	35	19	64.8
EfficientNetB4 + UNet	30	24	**55.6**	40	14	**74.1**

Recall, precision, sensitivity, and specificity were included in the RWMA assessment model, and they were 0.826, 0.817, 0.826, and 0.966, respectively. The results are presented in Table 3.

CAM was implemented to identify the area in which the RWMA model was focused. Figure 7 shows the CAM results of the RWMA model for each class. The CAM apical/anterior

Table 3
Recall, precision, sensitivity, and specificity evaluation results.

	Apical anterior	Basal	Septal	Normal	Average
Recall	0.947	0.857	0.5	1	0.826
Precision	0.857	1	0.5	0.909	0.817
Sensitivity	0.947	0.857	0.5	1	0.826
Specificity	0.909	1	0.98	0.976	0.966

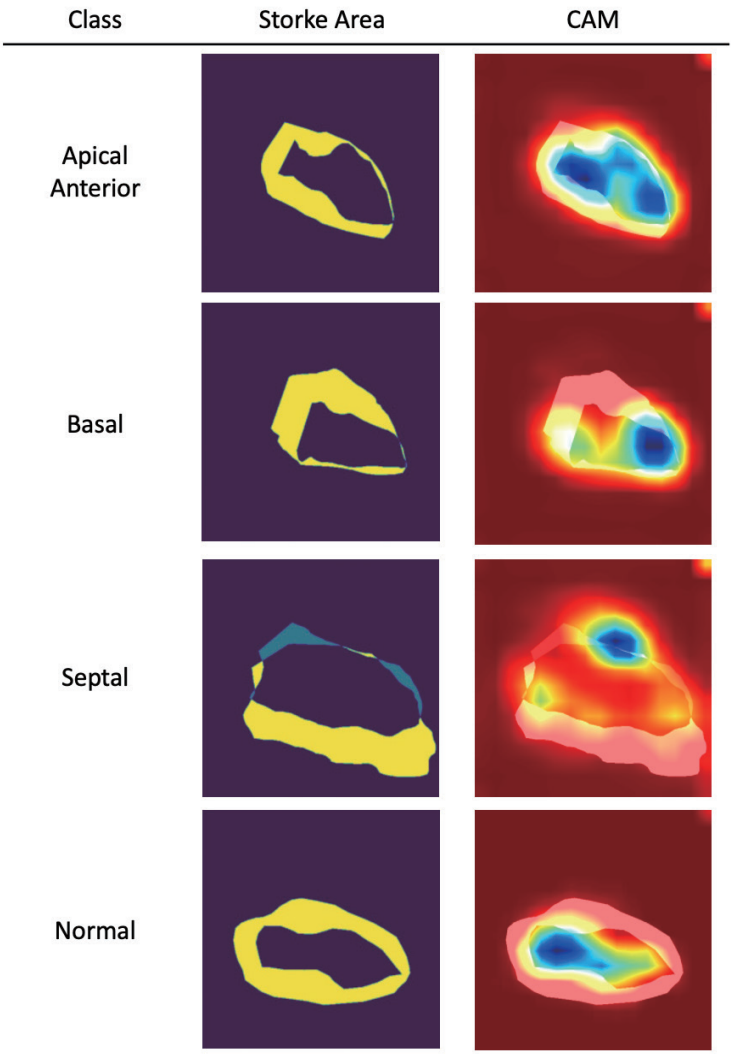

Fig. 7. (Color online) CAM results of the RWMA model.

area was focused on myocardial segments 2, 3, and 5 (blue and green areas). The CAM basal area was focused on myocardial segments 3, 4, and 5 (blue and green areas). The CAM septal area was focused on myocardial segments 1 and 2 (blue and green areas). The normal area was focused on the end-systolic area (blue and green areas).

5. Discussion

Echocardiography is widely adopted for EF measurement and RWMA assessment. Deep neural networks are also implemented in RWMA recognition. However, LVG is the gold standard for clinical diagnosis. The implementation of EF measurement through the adoption of semantic segmentation neural networks improves the measurement performance and provides automated EF measurement results. The state-of-the-art RWMA assessment method proposed in this study improved the RWMA recognition accuracy.

6. Conclusions

In this study, we proposed a novel method in which semantic segmentation neural networks were implemented for EF measurement. This method provided efficient and automated EF measurements for clinical diagnosis. Data set labeling and collection without clinicians are advantages of our proposed method. The mIoU value of our method had a maximum of 0.9215.

We also proposed a high-accuracy prediction method for RWMA assessment. Four classes (apical/anterior, basal, septal, and normal) were adopted. The sensitivity and specificity values were 0.826 and 0.966, respectively.

References

1 R. R. Selvaraju, M. Cogswell, A. Das, R. Vedantam, D. Parikh, and D. Batra: IEEE Int. Conf. Computer Vision (ICCV, 2017) 618. https://doi.org/10.1109/ICCV.2017.74
2 M. Cikes and S. D. Solomon: Eur. Heart J. **37** (2016) 1642. https://doi.org/10.1093/eurheartj/ehv510
3 P. W. Wood, J. B. Choy, N. C. Nanda, and H. Becher: Echocardiography **31** (2014) 87. https://doi.org/10.1111/echo.12331
4 C. Asferg, L. Usinger, T. S. Kristensen, and J. Abdulla: Eur. J. Radiol. **81** (2012) 757. https://doi.org/10.1016/j.ejrad.2012.02.002
5 M. Abe, Y. Kazatani, H. Fukuda, H. Tatsuno, H. Habara, and H. Shinbata: J. Nucl. Cardiol. **7** (2000) 569. https://doi.org/10.1067/mnc.2000.108607
6 M. Motwani, D. S. Berman, G. Germano, and P. Slomka: Cardiol. Clin. **34** (2016) 47. https://doi.org/10.1016%2Fj.ccl.2015.08.003
7 F. J. Wackers, H. J. Berger, D. E. Johnstone, L. Goldman, L. A. Reduto, R. A. Langou, A. Gottschalk, and B. L. Zaret: Am. J. Cardiol. **43** (1979) 1159. https://doi.org/10.1016/0002-9149(79)90148-6
8 Y. Koyama, T. Mochizuki, and J. Higaki: J. Magn. Reason. Imaging **19** (2004) 800. https://doi.org/10.1002/jmri.20067
9 P. Ponikowski, A. A. Voors, S. D. Anker, H. Bueno, J. G. F. Cleland, A. J. S. Coats, V. Falk, J. R. González-Juanatey, V. Harjola, E. A. Jankowska, M. Jessup, C. Linde, P. Nihoyannopoulos, J. T. Parissis, B. Pieske, J. P. Riley, G. M. C. Rosano, L. M. Ruilope, F. Ruschitzka, F. H. Rutten, P. V. D. Meer, and ESC Scientific Document Group: Eur. Heart J. **37** (2016) 2129. https://doi.org/10.1093/eurheartj/ehw128
10 K. Kusunose, A. Haga, N. Yamaguchi, T. Abe, D. Fukuda, H. Yamada, M. Harada, and M. Sata: J. Am. Soc. Echocardiogr. **33** (2020) 632. https://doi.org/10.1016/j.echo.2020.01.009
11 T. Kim, M. Hedayat, V. V. Vaitkus, M. Belohlavek, V. Krishnamurthy, and I. Borazjani: Quant. Imaging Med. Surg. **11** (2021) 1763. https://doi.org/10.21037/qims-20-745

12 K. Suzuki, I. Horiba, N. Sugie, and M. Nanki: IEEE Trans. Med. Imaging **23** (2004) 330. https://doi.org/10.1109/tmi.2004.824238
13 M. S. Huang, C. S. Wang, J. H. Chiang, P. Y. Liu, and W. C. Tsai: Circulation **142** (2020) 1510. https://doi.org/10.1161/CIRCULATIONAHA.120.047530
14 Y. Y. Chen, G. Y. Li, S. Y. Jhong, P. H. Chen, C. C. Tsai, and P. H. Chen: Sens. Mater. **32** (2020) 3157. https://doi.org/10.18494/SAM.2020.2838
15 C. J. Lin, Y. C. Li, and C. L. Lee: Sens. Mater. **31** (2019) 159. https://doi.org/10.18494/SAM.2019.2577
16 X. Zhang, H. Huang, W. Meng, and D. Luo: Sens. Mater. **32** (2020) 4505. https://doi.org/10.18494/SAM.2020.3128
17 K. Wada: labelme, https://github.com/wkentaro/labelme (accessed July 2021).
18 O. Ronneberger, P. Fischer, and T. Brox: Med. Image Comput. Comput. Assist. Interv. **9351** (2015) 234. https://doi.org/10.1007/978-3-319-24574-4_28
19 M. Tan and Q. V. Le: EfficientNet: Rethinking Model Scaling for Convolutional Neural Networks (2019). arXiv:1905.11946v5
20 K. He, G. Gkioxari, P. Dollár, and R. Girshick: IEEE Int. Conf. Computer Vision (ICCV, 2017) 2961–2969. https://doi.org/10.1109/ICCV.2017.322